IEEE Photonics Journal
An IEEE Photonics Society Publication

Open Access

Multiple-Image Hiding by Using Single-Shot Ptychography in Transform Domain

Volume 9, Number 3, June 2017

Wenhui Xu
Yong Luo
Tuo Li
Huaying Wang
Yishi Shi

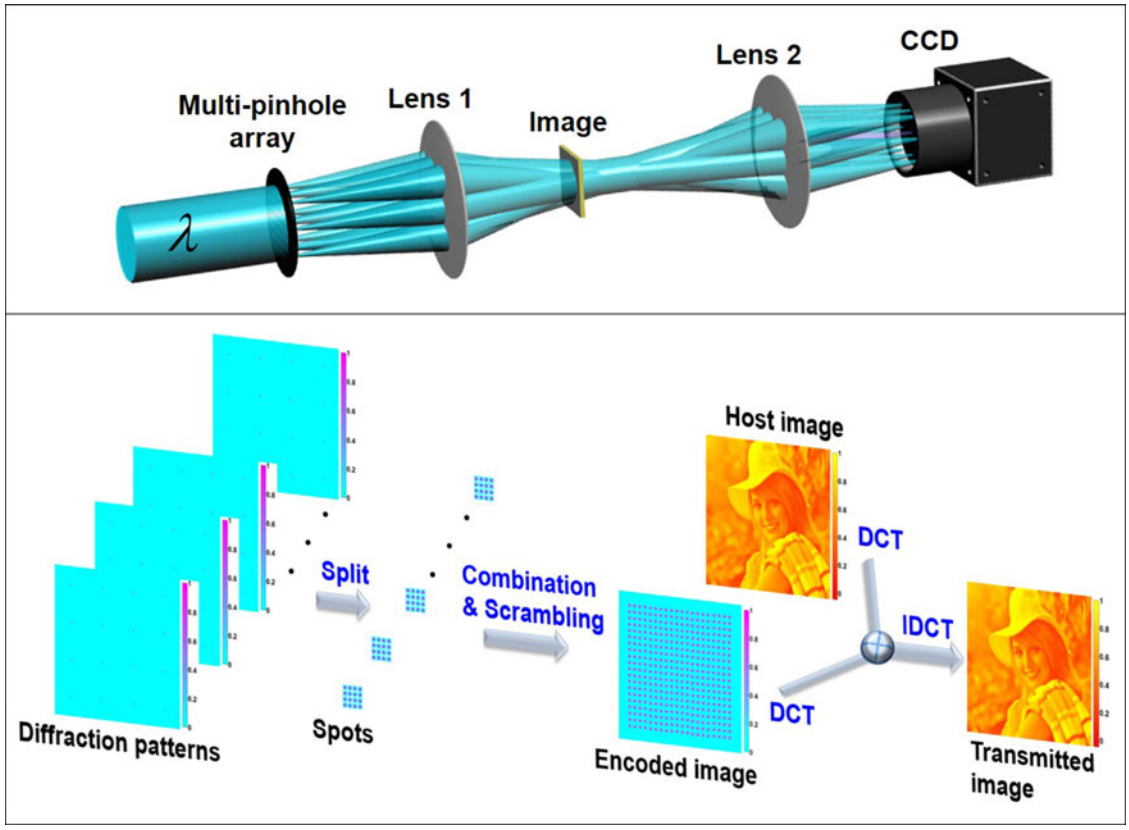

DOI: 10.1109/JPHOT.2017.2695398
1943-0655 © 2017 IEEE

Multiple-Image Hiding by Using Single-Shot Ptychography in Transform Domain

Wenhui Xu,[1,2] Yong Luo,[1,2] Tuo Li,[3] Huaying Wang,[4] and Yishi Shi[1,2]

[1]College of Materials Science and Opto-Electronic Technology, University of Chinese Academy of Sciences, Beijing 100049, China
[2]Academy of Opto-Electronics, Chinese Academy of Sciences, Beijing 100094, China
[3]Department of Applied Statistics and Science, Xijing University, Xi'an 710123, China
[4]College of Mathematics and Physics, Hebei University of Engineering, Handan 056038, China

DOI:10.1109/JPHOT.2017.2695398

Manuscript received January 11, 2017; revised March 26, 2017; accepted April 14, 2017. Date of current version April 26, 2017. This work was supported in part by the National Natural Science Foundation of China under Grant 61575197; in part by the K. C. Wong Education Foundation; in part by the Fusion Foundation of Research and Education, Chinese Academy of Sciences (CAS); in part by the Youth Innovation Promotion Association CAS; and in part by the International Science and Technology Cooperation under Grant 2014DFE00200. Corresponding author: Y. Shi (e-mail: optsys@gmail.com).

Abstract: A practical method using single-shot ptychographic imaging (SPI) in the transform domain is proposed for multiple-image hiding. The excellent compressibility of SPI can bring high multiplexing capacity and imperceptibility to the proposed multiple-image hiding system. The security is mainly supported by the imperceptibility and the large quantity of scrambling modes, and security will be improved greatly with the increase of hidden images. Furthermore, the successful combination with the discrete cosine transform-domain algorithm can not only further enhance the imperceptibility and security but indicates that SPI-based multiple-image hiding is compatible with transform domain algorithms as well. Optical experiments demonstrate the high feasibility, multiplexing capacity, imperceptibility, and security of the proposed technique. The proposed method may open up a novel research perspective for multiple-image hiding combined with various efficient transform domain algorithms.

Index Terms: Optical multiple-image hiding, single-shot ptychography, transform domain.

1. Introduction

As one of the most attractive issues, multiple-image hiding has been widely applied in multiple-user authentications and copyright protection [1]. Since double-random phase encoding (DRPE) is proposed in 1995 [2], massive extension strategies for multiple-image encryption and hiding have been proposed [3]–[10]. Plenty of those methods are based DRPE, such as wavelength multiplexing [3], information prechoosing [4], and cascaded phase retrieval algorithm [5]. Those DRPE-based systems utilize two independent random phase masks, which requires extremely accurate alignment in the optical setup to ensure the high quality description. The high alignment precision makes it greatly hard to carry out the optical experiment. Besides, many multiple-image encryption and hiding techniques have been implemented by designing phase-only masks [6]–[10], in which the cross-talk terms can be suppressed significantly. However, those methods

need complicated process to manufacture the encoded multiple phase masks, which limits the extensive application in the practice. It urgently requires to design an optical system that can keep a balance between hiding capacity, security, and experimental feasibility.

In this paper, we propose a practical multiple-image hiding method by use of single-shot ptychographic imaging (SPI) in transform domain. SPI is a newly proposed coherent diffraction imaging technique [11]–[13], which has the similar illumination method to ptychography [14]–[20]. Different from ptychography-based encryption [21], our proposed method can not only capture a diffraction pattern in a single exposure, but also requires no mechanical scanning and random phase masks. In SPI, since a complex-valued object is encoded into a diffraction pattern constituted by lots of almost invisible tiny spots, SPI has excellent compressibility and imperceptibility. We just extract massive tiny spots corresponding to multiple images with nearly lossless operation, and scramble those tiny spots in a jigsaw method [22]. The more hidden images are, the higher security will be. The imperceptibility, and large amount of scrambling modes can support the security powerfully. In addition, the ample structural parameters (λ, f_1, f_2, d) and diversity of the multi-pinhole array can also be severed as keys [13]. To further improve the above properties of this hiding system and test that SPI-based multiple image hiding can be extensively applied in transform domain, we embed the encoded image in the discrete cosine transform (DCT) domain [23], [24]. The embedding process can also be operated in other transform domain, such as discrete Fourier transform [25], and discrete wavelet transform [26]. Compared with spatial-domain hiding techniques, transform domain methods can increase the imperceptibility and security, as well as further compress the encoded image. We have performed optical experiment to demonstrate the high multiplexing capacity, imperceptibility, and security of SPI-based multiple-image hiding system in transform domain.

2. Theoretical Analysis

2.1 SPI-Based Multiple-Image Hiding in Transform Domain

The proposed multiple-image hiding system is illustrated in Fig. 1, and the general hiding process is shown in Fig. 2(a). Fig. 1(a) shows the schematic of SPI, which is first part of the hiding system and also acting as the core, the properties of SPI makes it suitable for multiple-image hiding. The ray tracing elementary diagram of SPI is shown in Fig. 1(b). Fig. 1(c) displays the second part of the hiding system, which makes full use of the characteristics of SPI to achieve high multiplexing capacity and security.

In Fig. 1(a), numbers of complex-valued images are encrypted into some diffraction patterns with pretty imperceptibility and compressibility. One of the image we wish to encrypt is placed at distance $d \neq 0$ before or after the Fourier plane of the $4f$ system. A plate of $N \times N$ multi-pinhole square array ($N = 4$ in our experiment) is located at the input plane of the $4f$ system, the diameter of the circular pinhole is D, and the distance between the consecutive pinholes is b. Firstly, A plane wave is divided into $N \times N$ beams through the multi-pinhole array, these consecutive beams overlap with each other in a certain region between Lens 1 and Lens 2. $N \times N$ probes U illuminating on the complex-valued image are generated simultaneously:

$$\begin{aligned} U &= \sum_n U_n \\ &= \sum_n \left(\xi_{(f_1-d)}[\xi_{f_1}[P(r-R_n)]\cdot t]\right), (n = 1, 2, \cdots, N^2) \end{aligned} \tag{1}$$

where $\xi_d[\cdot]$ is the angular spectrum propagation with the distance d, $t = \exp[-j \cdot k/2f \cdot (x^2 + y^2)]$ is the quadratic phase factor applied to simulate the modulation of lens [27], [28], the $\sum_n P(r - R_n)$ stands for the $N \times N$ pinholes, R_n is the center of the n_{th} pinhole, and U_n is the n_{th} probe illuminating on the image. According to geometrical optics, we can deduce from the system shown in Fig. 1(b), the magnification of the 4f system is f_1/f_2, the distance between the adjacent illumination beams in the object plane is $\mathrm{r} = bd/f_1$. When N is large enough, the field of view (FOV) can be approximated as $\mathbf{FOV} = N\mathrm{r} = Nbd/f_1$ [11]. When $N = 4$, $b = 1.54$ mm, $d = 23$ mm, $f_1 = 75$ mm, and the size

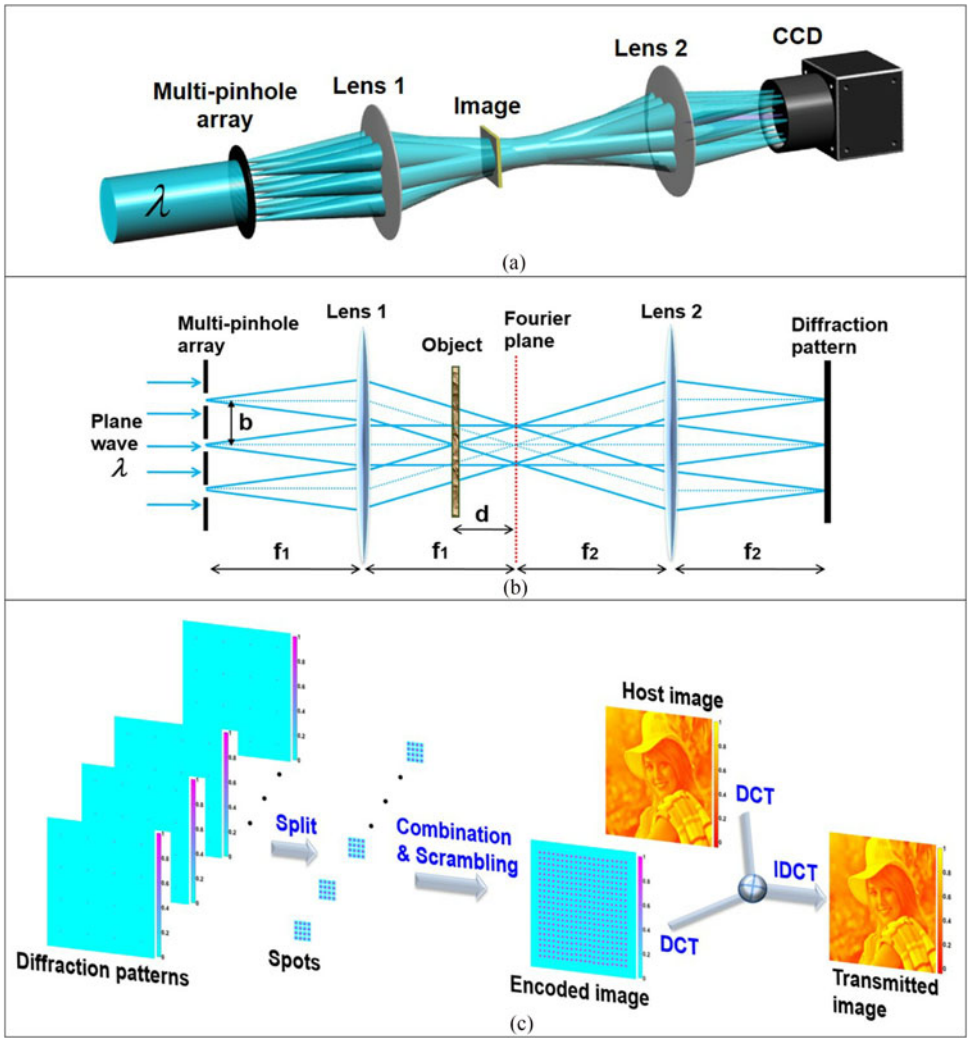

Fig. 1. Schematic setups for multiple-image hiding. (a) Schematic setup for single-shot ptychography. (b) Ray tracing elementary diagram of single-shot ptychography. b is the distance between the consecutive pinholes, and f_1 and f_2 are the focal distances of Lens1 and Lens2, respectively. The object is located at distance d before the back focal plane of Lens1, and the CCD is placed at the back focal plane of Lens2. (c) Schematic for the operation of diffraction patterns hiding. DCT and IDCT represents discrete cosine transform and inverse discrete cosine transform, respectively.

of each pixel is 5.5 $\times$ 5.5 μm, the FOV is about 3 mm. For an image with 1120 $\times$ 1120 pixels, the FOV is about 550 $\times$ 550 pixels, as shown in Fig. 2(b) and (c) respectively. Secondly, the diffraction pattern $IO_i (i = 1, 2, \ldots, M)$ corresponding to the i_{th} hidden image is recorded by the CCD located at the output plane of the 4f system:

$$I_n^i = \left|\xi_{f_2}(\xi_{(f_2+d)}[U_n \cdot f(x, y)] \cdot t)\right|^2 \tag{2}$$

$$IO_i = \sum_n I_n^i \tag{3}$$

where I_n^i is the n_{th} diffraction spot corresponding to the n_{th} pinhole for the i_{th} hidden image, and $f(x, y)$ is the complex-valued image. It is obvious that those diffraction patterns are constituted by numbers of tiny spots and that those spots are too weeny to be perceived by our naked eyes, which means that the diffraction pattern itself has strong imperceptibility.

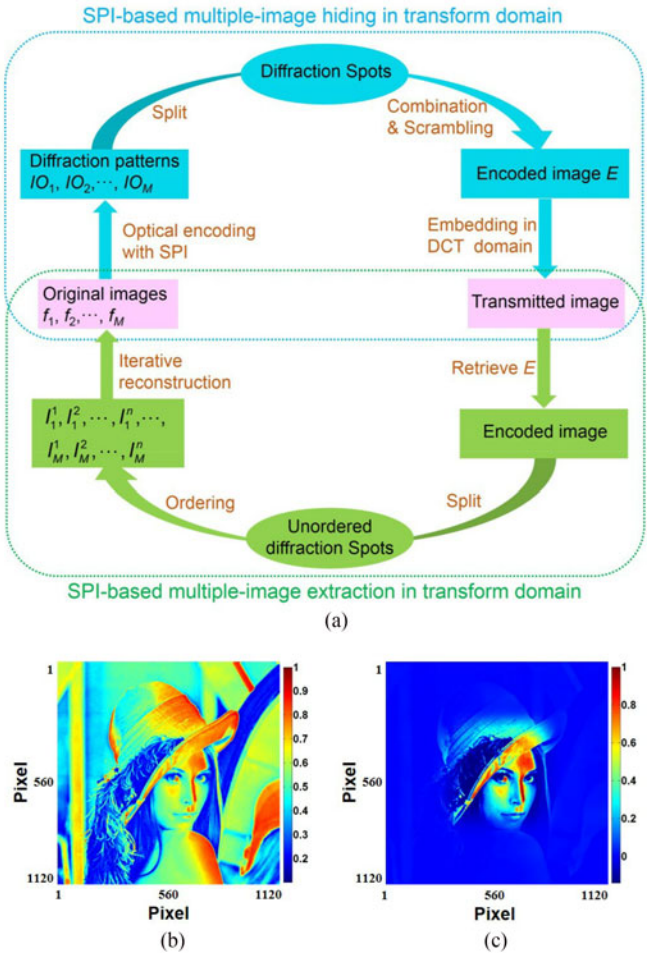

Fig. 2. (a) Flow chart for illustrating the hiding and extraction process. (b) Original image. (c) Image illuminated by multiple beams.

In Fig. 1(c), multiple diffraction patterns are embedded into a host image in the transform domain. Considering that those diffraction patterns are constituted by a set of tiny diffraction spots I_n^i, these tiny spots I_n^i are extracted to remove the data redundancy. The number of total spots is $M \times N^2$. The information of the image is mainly stored in these tiny spots, the other parts are just data redundancy. To acquire larger compression ratio and multiplexing capacity, we can improve FOV by increasing .. and decreasing f_1 properly. Then, we combine $M \times N^2$ spots together, and scramble all of the spots in a jigsaw method. When the distribution pattern [13] is square like the distribution of encoded image in Fig. 1(c), the amount of scrambling modes is $(M \times N^2)!$, let alone change the distribution patterns of those tiny spots, resulting that it is extremely difficult to recover the distribution of the whole diffraction patterns. The larger N and M are, the higher security will be. At last, the encoded image E obtained from the above steps is embedded into a host image H in DCT domain [24]. Apart from the applying of single-shot ptychography into multiple-image hiding, the embedding methods in transform domain is the key difference with [13]. The DCT is applied in blocks of 8×8 pixels, as in the JPEG algorithm [29]

$$TI = idct2(\text{dct2}(H) + \alpha \cdot dct2(E)) \tag{4}$$

where TI is the transmitted image, $dct2(\cdot)$ represents 2-D DCT, $idct2(\cdot)$ represents inverse 2-D DCT, and α is the perceptual mask, which is basically used to amplify or attenuate the encoded image at

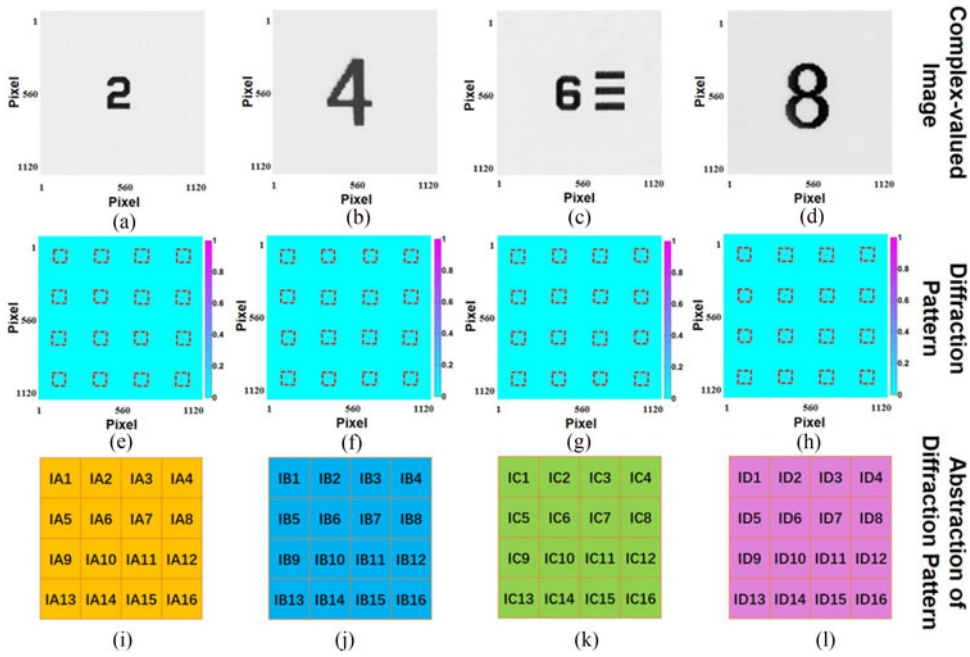

Fig. 3. (a)–(d) Complex-valued images used in the optical experiment. (e)–(h) Diffraction patterns recorded by CCD at the output plane of single-shot ptychography imaging system. (i)–(l) Abstraction of each diffraction pattern.

each DCT coefficient so that the hidden image energy is maximized while the alterations suffered by the image are kept invisible [24].

2.2 SPI-Based Multiple-Image Extraction in Transform Domain

The extraction of the complex-valued images is the inversion of the hiding of images, which is illustrated as Fig. 2(a). First, the encoded image is extracted from the transmitted image faultlessly. Second, the diffracton patterns I_n^i are arranged into right distribution patterns and orders. Finally, the phase and amplitude of the image can be reconstructed with the standard PIE algorithm [30]. The above process can be described as follows:

1) Extract the encoded image E, and

$$E = idct2(\mathrm{dct2}(TI) - dct2(H)). \tag{5}$$

2) Split the encoded image E into $M \times N^2$ spot blocks, and then arrange these patterns I_n^i in the correct distribution modes.
3) For each image, guess the complex value of the input image $f_g^i(x, y)$, and then begin the following iterative process.
4) In the m_{th} iteration, $f_{ng}^{im}(x, y)$ is illuminated by the n_{th} probe, and the intensity I_{ng}^{im} is acquired at the output plane of the $4f$ system:

$$I_{ng}^{im} = \left|\xi_{f_2}(\xi_{(f_2+d)}[U_n \cdot f_{ng}^{im}(x, y)] \cdot t)\right|^2. \tag{6}$$

5) Substitute the amplitude term of I_{ng}^{im} with the recorded pattern I_n^i, while preserving the phase:

$$I_n^{im} = \begin{cases} \sqrt{I_n^i} \cdot \left[I_{ng}^{im} / \left|I_{ng}^{im}\right|\right], & r \notin \gamma \\ I_{ng}^{im}, & r \in \gamma \end{cases} \tag{7}$$

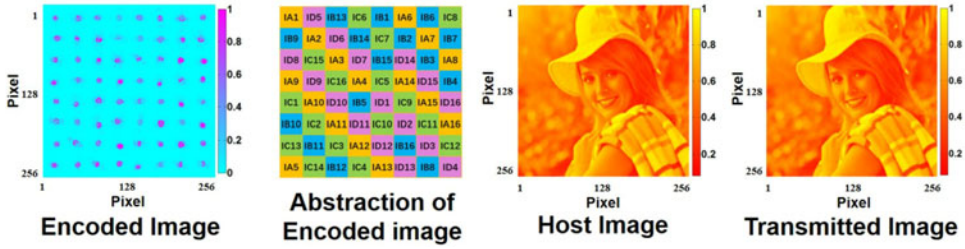

Fig. 4. (a) Final encoded image (256 × 256 pixels). (b) Abstraction of encoded image. (c) Host image (256 × 256 pixels). (d) Transmitted image (256 × 256 pixels).

where r represents the pixel value of I_n^i, and γ is the pixel in the saturated section of I_n^i. The I_n^i we recorded is partially saturated, and the reconstruction quality can be enhanced in this way according to the analysis in [31].

6) Take the inverse transform of I_n^{im} to the object plane:

$$f_{ngNew}^{im}(x,y) = \xi_{(f_2+d)}^{-1}[\xi_{f_2}^{-1}(I_n^{im}) \cdot t^*] \tag{8}$$

where t^* is the conjugate of t.

7) Renew $f_{(n+1)g}^{im}(x+y)$ with $f_{ngNew}^{im}(x,y)$ according to

$$\begin{aligned} f_{(n+1)g}^{im}(x+y) &= f_{ng}^{im}(x+y) \\ &+ \frac{U_n^*}{\max(|U_n|^2)} \cdot (f_{ngNew}^{im}(\mathrm{x},\mathrm{y}) - U_n \cdot f_{ng}^{im}(\mathrm{x},\mathrm{y})) \end{aligned} \tag{9}$$

where U_n^* is the conjugate of U_n.

8) Repeat the above steps 4 through 6 for $N \times N$ separate patterns to complete an entire iteration.
9) Repeat the above steps 2 through 7 for M images.
10) Calculate the peak signal to noise ratio (PSNR), which is usually used to measure the image quality [32], [33],

$$\mathrm{PSNR} = 10 \cdot log_{10}(\mathrm{MaxPV}/\mathrm{MSE})(dB) \tag{10}$$

$$\mathrm{MSE} = \left(\sum_{p=1}^{P} \sum_{q=1}^{Q} (f_{p,q} - f'_{p,q}) \right) / (\mathrm{P} \cdot Q) \tag{11}$$

where MSE is the mean squared error, and $f_{p,q}$ and $f'_{p,q}$ are the original and the transmitted images, respectively. The size of $f_{p,q}$ and $f'_{p,q}$ are $P \times Q$, and the maximum pixel value of the image is $MaxPV$.

3. Experimental Results and Analysis

We have performed the optical experiment to demonstrate that our proposed SPI-based multiple-image hiding technique can make a well balance between multiplexing capacity, security and experimental feasibility. In our optical experiment, the wavelength of the laser is $\lambda = 473$ nm, the focal distances of Lens 1 and Lens 2 are $f_1 = f_2 = 75$ mm. The pixel size of the CCD is 5.5 μm. The multi-pinhole array is a 4×4 square array, the diameter D of the circular pinhole is 49.5 μm, and the distance b between consecutive pinholes is 1.54 mm. The complex-valued image is placed at a distance $d = 23$ mm before the Fourier plane of the $4f$ system. For brevity, we just take four images as examples. Fig. 4(a)–(d) show the secret multiple images, which are transparent object with figures of 2, 4, 6, and 8 captured by a general camera with 8× magnification, and the figures of 4 and 8 are nearly 2 times bigger than 2 and 6.

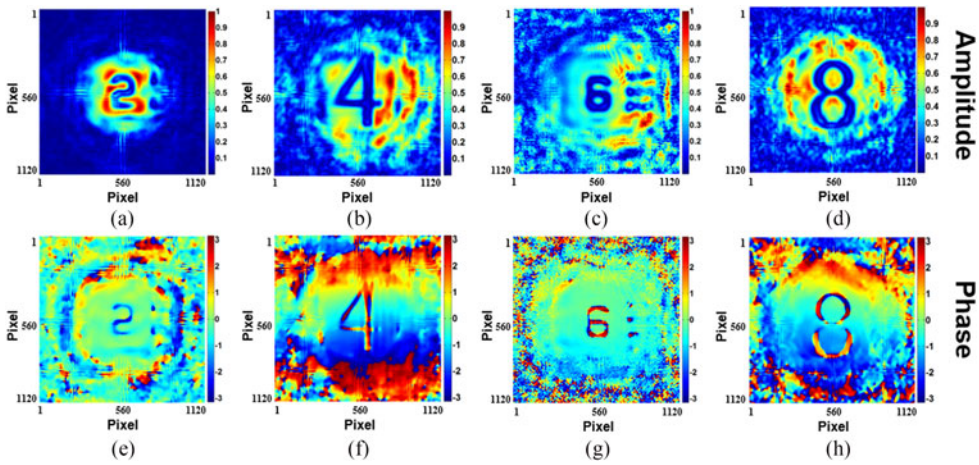

Fig. 5. Extracted complex-valued images (1120 × 1120 pixels). (a)–(d) Amplitude distributions. (a)–(d) Amplitude distributions.

3.1 Multiplexing Capacity

Optical experiment results show that the compressibility of SPI makes our proposed multiple-image hiding system have high multiplexing capacity. The diffraction patterns corresponding to these images are shown as Fig. 3(e)–(h), respectively. In the phase retrieval algorithm, the size of each diffraction pattern in the optical system is 1120 × 1120 pixels. To distinguish the spots (marked in red dotted blocks) of different diffraction pattern, we mark these spots in an abstract way. IA1, ⋯, IA16, IB1, ⋯, IB16, IC1, ⋯, IC16, and ID1, ⋯, ID16 represent the diffraction spots of objects 2, 4, 6, 8, respectively, as shown in Fig. 3(i)–(l). In those diffraction patterns, the information of the objects is mainly stored in the tiny spots, some high-frequency components distribute around these spots, it can be clearly seen from Fig. 4(a), in which the diameters of diffraction spots are magnified about 4 times. We extract all of the tiny spots from the four diffraction patterns to obtain reconstruction quality, the extracted length of each spot block should be no less than 28 pixels, and the using length in this experiment is 30 pixels. Then, these spot blocks are combined together and scrambled as shown in Fig. 4(b).

In our proposed multiple-image hiding system, the multiplexing capacity is depended on the structures of multi-pinhole array and imaging system, as well as the size of the host image. Since that the diffraction spot is determined by the size of pinhole and the magnification of the 4f system, M is mainly limited by the size of host image when the structures of multi-pinhole array and imaging system are constant. In ptychography-based encryption and hiding [21], [34], the object is illuminated by multiple partially overlapping beams with times of mechanical scanning, respectively. For an image with 256 × 256 pixels, it is encrypted into 16 diffraction patterns with 16 steps mechanical scanning. It requires 16 × 4 host images to hide the diffraction patterns of 4 original images. That is to say, the large data redundancy causes the low multiplexing capacity. In single-shot ptychography, multiple partially overlapping beams illuminated on the image simultaneously without mechanical scanning. In our experiment, the length of the extracted tiny diffraction spots blocks is 30 pixels, the whole size of 16 tiny spots is 120 × 120 pixels, a host image with 256 × 256 pixels can hide at least 4 images. Fig. 4(a), (c) and (d) are the final encoded image, host image and transmitted image respectively, the sizes of which are all 256 × 256 pixels. Fig. 5 shows that the complex-valued images are extracted successfully, Fig. 5(a)–(d) and (e)–(h) are reconstructed amplitude and phase distributions, respectively. It is obvious that reconstructed amplitude and phase distributions of three bars aside the Fig. 6 can be recognized clearly, which shows the good extracted quality. Further, the increasing of multiplexing capacity M has no influence on the performance of the extracted complex-valued images. The multiplexing capacity is 64 times larger

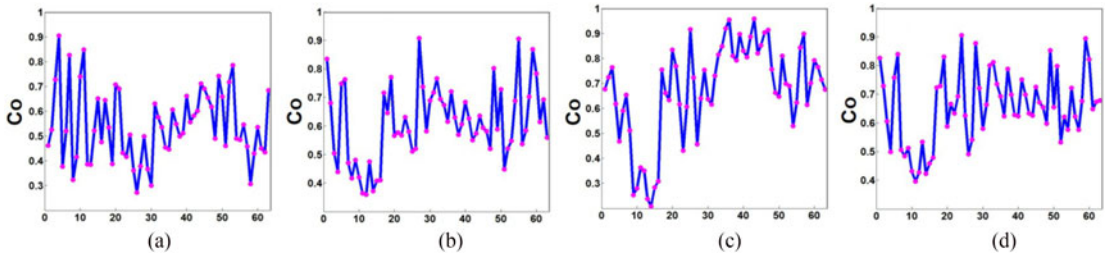

Fig. 6. Correlation coefficient *Co* between one spot block with other 63 spot blocks. (a) *Co* between IA8 with other 63 spot blocks (from IA1 . . . IA7, IA9 . . . IA16, IB1 . . . IB16, IC1 . . . IC16, to ID1 . . . ID16). (b) *Co* between IB8 with other 63 spot blocks (from IA1 . . . IA16, IB1 . . . IB7, IB9 . . . IB16, IC1 . . . IC16, to ID1 . . . ID16). (c) *Co* between IC8 with other 63 spot blocks (from IA1 . . . IA16, IB1 . . . IB16, IC1 . . . IC7, IC9 . . . IC16, to ID1 . . . ID16). (d) *Co* between ID8 with other 63 spot blocks (from IA1 . . . IA16, IB1 . . . IB16, IC1 . . . IC16, to ID1 . . . ID7, ID9 . . . ID16).

than traditional PI-based hiding, which means that our proposed multiple-image hiding system has extremely large multiplexing capacity.

3.2 Imperceptibility

The combination with DCT-domain embedding algorithm and the inherent compressibility of SPI make the proposed method has high imperceptibility. Compared with [13], the imperceptibility can be further enhanced by the introduction of embedding methods in transform domain, only the results with DCT domain are presented for brevity. The diameter of one tiny diffraction spot is about 49.5 μm, it is too difficult to identify it by our naked eyes, as shown in Fig. 3(e)–(h). Further, the diameter of these tiny spots can be decreased to less than 10 μm by adjusting the structural parameters (the size of pinhole, f_1, and f_2), those tiny spots are almost invisible before the operation of attenuation. To further improve the imperceptibility, the embedding of the encoded image into host image has been performed in DCT domain, the host image and the final transmitted image are shown in Fig. 4(c) and (d). The value of *PSNR* between transmitted image and host image is 56.5114 dB, and we cannot distinguish the transmitted image and host image by our naked eyes. We cannot distinguish the transmitted image and host image by our naked eyes. The value of *PSNR* between transmitted image and host image is 56.5114 dB, and it has been demonstrated that the *PSNR* should be kept more than 35 dB for good embedding performance [35]. It indicates that SPI-based multiple-image hiding system has strong imperceptibility.

3.3 Security

The security of the proposed method is mainly supported by the strong imperceptibility and the large amount of scrambling modes. In single-shot ptychography, the position of each tiny spot in the diffraction pattern is strictly fixed. Each diffraction spot is solely corresponding to an illumination beam that illuminates on a certain area of the object. We scramble those tiny spots by a simple jigsaw method, and change the distribution patterns and orders of those tiny spots discretionarily, as shown in Fig. 1(c). The complex-valued image cannot be reconstructed, when the distribution pattern and orders of those spots are scrambled. We have calculated correlation coefficient *Co* between the spot block (IA8, IB8, IC8, or ID8) with other 63 spot blocks (from IA1 $\cdots$ IA16, IB1 $\cdots$ IB16, IC1 $\cdots$ IC16, to ID1 $\cdots$ ID16), respectively, as shown in Fig. 6(a)–(d). Fig. 6 illustrates that the distributions of those spots cannot be returned to their initial state by calculating the *Co* between all of the spots. The multi-pinhole array we use in the paper is a 4×4 square array, each diffraction pattern can be compressed into 16 discrete spots blocks, as shown in Fig. 3(e)–(h). When diffraction pattern of all spots blocks are arranged as the square array shown in Fig. 4(a), the amount of scrambling modes is $(4 \cdot 16)! \approx 1.269 \cdot 10^{89}$, let alone change the distribution patterns of those tiny spots, resulting

that it is extremely difficult to recover the distribution of diffraction pattern [13]. The larger N and M are, the higher security will be. M and N should be optimized according to the structure of imaging system, the size of host image and the performance of computer. In addition, as can be easily deduced from Fig. 1(b), all of the system structural parameters (λ, f_1, f_2, d) and the diversity of the multi-pinhole array can be served as keys, the diversity includes the distribution pattern of the array, the shape and size of the pinhole, and the distance b between the consecutive pinholes. All of these form a large key space, the security of our proposed multiple-image hiding system can be guaranteed, and the security can also be improved constantly by increasing the number of pinholes and decreasing the size of diffraction spots.

4. Conclusion

We have proposed a novel multiple-image hiding method using SPI in transform domain. Since the images are compressed into a series of discrete tiny spots by SPI, the inherent compressibility makes it suitable for multiple-image hiding. On the one hand, the high multiplexing capacity and imperceptibility can be brought by the remarkable compressibility. On the other hand, the security can be powerfully supported by the imperceptibility and the large quantity of scrambling modes. To further improve the imperceptibility and security, SPI-based multiple-image hiding is combined with DCT-domain algorithm. Optical experiment validates the high multiplexing capacity, imperceptibility, and security of the proposed technique, which may promote the practicality of optical security.

References

[1] I. J. Cox, M. L. Miller, and J. A. Bloom, *Digital Watermarking and Fundamentals*. San Francisco, CA, USA: Morgan Kaufmann, 2002.
[2] P. Refregier and B. Javidi, "Optical image encryption based on input plane and Fourier plane random encoding," *Opt. Lett.*, vol. 20, pp. 767–769, 1995.
[3] G. Situ and J. Zhang, "Multiple-image encryption by wavelength multiplexing," *Opt. Lett.*, vol. 30, pp. 1306–1308, 2005.
[4] Y. Shi, G. Situ, and J. Zhang, "Multiple-image hiding by information prechoosing," *Opt. Lett.*, vol. 33, pp. 542–544, 2008.
[5] Y. Xiao, X. Zhou, S. Yuan, Q. Liu, and Y. Li, "Multiple-image optical encryption: An improved encoding approach," *Appl. Opt.*, vol. 48, pp. 2686–2692, 2009.
[6] W. Chen, "Optical multiple-image encryption using three-dimensional space," *IEEE Photon. J.*, vol. 8, no. 2, Apr. 2016, Art. no. 6900608.
[7] W. Chen and X. Chen, "Optical multiple-image encryption based on multiplane phase retrieval and interference," *J. Opt.*, vol. 13, 2011, Art. no. 115401.
[8] Y. Shi, G. Situ, and J. Zhang, "Multiple-image hiding in the Fresnel domain," *Opt. Lett.*, vol. 32, pp. 1914–1916, 2007.
[9] X. Li *et al.*, "Multiple-image encryption based on compressive ghost imaging and coordinate sampling," *IEEE Photon. J.*, vol. 8, no. 4, Aug. 2016, Art. no. 3900511.
[10] W. He, X. Peng, and X. Meng, "Optical multiple-image hiding based on interference and grating modulation," *J. Opt.*, vol. 14, 2012, Art. no. 075401.
[11] P. Sidorenko and O. Cohen, "Single-shot ptychography," *Optica*, vol. 3, pp. 9–14, 2016.
[12] X. Pan, C. Liu, and J. Zhu, "Single shot ptychographical iterative engine based on multi-beam illumination," *Appl. Phys. Lett.*, vol. 103, 2013, Art. no. 171105.
[13] W. Xu, H. Xu, Y. Luo, T. Li, and Y. Shi, "Optical watermarking based on single-shot-ptychography encoding," *Opt. Exp.*, vol. 24, pp. 27922–27936, 2016.
[14] J. M. Rodenburg, "Ptychography and related diffractive imaging methods," *Adv. Imag. Electron Phys.*, vol. 150, pp. 87–184, 2008.
[15] A. M. Maiden, J. M. Rodenburg, and M. J. Humphy, "Optical ptychography: A practical implementation with useful resolution," *Opt. Lett.*, vol. 35, pp. 2585–2587, 2010.
[16] K. Guo, S. Dong, and G. Zheng, "Fourier ptychography for brightfield, phase, darkfield, reflective, multi-slice, and fluorescence imaging," *IEEE J. Sel. Topics Quantum Electron.*, vol. 22, no. 4, Jul./Aug. 2016, Art. no. 6802712.
[17] Q. Gao, Y. Wang, T. Li, and Y. Shi, "Optical encryption of unlimited-size images based on ptychographic scanning digital holography," *Appl. Opt.*, vol. 53, pp. 4700–4707, 2014.
[18] Y. Shi, Y. Wang, and S. Zhang, "Generalized ptychography with diverse probes," *Chin. Phys. Lett.*, vol. 30, 2013, Art. no. 054203.
[19] H. M. L. Faulkner and J. M. Rodenburg, "Movable aperture lensless transmission microscopy: A novel phase retrieval algorithm," *Phys. Rev. Lett.*, vol. 93, 2004, Art. no. 023903.
[20] T. Li and Y. Shi, "Vulnerability of impulse attack-free four random phase mask cryptosystems to chosen-plaintext attack," *J. Opt.*, vol. 18, 2016, Art. no. 035702.
[21] Y. Shi, T. Li, Y. Wang, Q. Gao, S. Zhang, and H. Li, "Optical image encryption via ptychography," *Opt. Lett.*, vol. 38, pp. 1425–1427, 2013.

[22] P. Kumar, J. Joseph, and K. Singh, "Optical image encryption using a jigsaw transform for silhouette removal in interference-based methods and decryption with a single spatial light modulator," *Appl. Opt.*, vol. 50, pp. 1805–1811, 2011.
[23] M. A. Suhail and M. S. Obaidat, "Digital watermarking-based DCT and JPEG model," *IEEE Trans. Instrum. Meas.*, vol. 52, no. 5, pp. 1640–1647, Oct. 2003.
[24] J. R. Hernandez, M. Amado, and F. Perez-Gonzalez, "DCT-domain watermarking techniques for still images: detector performance analysis and a new structure," *IEEE Trans. Image Process.*, vol. 9, no. 1, pp. 55–68, Jan. 2000.
[25] M. Urvoy, D. Goudia, and F. Autrusseau, "Perceptual DFT watermarking with improved detection and robustness to geometrical distortions," *IEEE Trans. Inf. Forensics Secur.*, vol. 9, no. 7, pp. 1108–1119, Jul. 2014.
[26] N. M. Makbol, B. E. Khoo, and T. H. Rassem, "Block-based discrete wavelet transform-singular value decomposition image watermarking scheme using human visual system characteristics," *IET Image Process.*, vol. 10, pp. 34–52, 2016.
[27] E. Hecht, *Optics*, 4th ed. Reading, MA,USA: Addision-Wesley, 2001.
[28] W. Chen, "Correlated-photon secured imaging by iterative phase retrieval using axially-varying distances," *IEEE Photon. Technol. Lett.*, vol. 28, no. 18, pp. 1932–1935, Sep. 2016.
[29] G. K. Wallace, "The JPEG still picture compression standard," *IEEE Trans. Consum. Electron.*, vol. 38, no. 1, pp. 18–34, Feb. 1992.
[30] A. M. Maiden and J. M. Rodenburg, "An improved ptychographical phase retrieval algorithm for diffractive imaging," *Ultramicroscopy*, vol. 109, pp. 1256–1262, 2009.
[31] X. Pan, S. P Veetil, B. Wang, C. Liu, and J. Zhu, "Ptychographical imaging with partially saturated diffraction patterns," *J. Mod. Opt.*, vol. 62, pp. 1270–1277, 2015.
[32] A. Poljicak, L. Mandic, and D. Agic, "Discrete Fourier transform- based watermarking method with an optimal implementation radius," *J. Electron. Imag.*, vol. 20, 2011, Art. no. 033008.
[33] W. Chen, "Optical cryptosystem based on single-pixel encoding using the modified Gerchberg–Saxton algorithm with a cascaded structure," *J. Opt. Soc. Amer. A.*, vol. 33, pp. 2305–2311, 2016.
[34] J. Zhang, Z. Wang, T. Li, A. Pan, Y. Wang, and Y. Shi, "3D object hiding using three-dimensional ptychography," *J. Opt.*, vol. 18, 2016, Art. no. 095701.
[35] D. Bhowmik and C. Abhayaratne, "On robustness against JPEG2000: A performance evaluation of wavelet-based watermarking techniques," *Multimedia Syst.*, vol. 20, pp. 239–252, 2014.